ARPN Journal of Engineering and Applied Sciences




# STUDY OF MECHANICAL PROPERTIES UNDER DIFFERENT COOLING CONDITIONS OF JIS G3141 SPCC STEEL COATED BY WIRE ARC SPRAY

Montri Sangsuriyun
Department of Industrial Engineering, Nakhon Phanom University, Nakhon Phanom, Thailand
E-Mail: montri.sang@npu.ac.th

**ABSTRACT**

The objectives of this study were to improve the surface hardness of specimens and maintenance of JIS G3141 SPCC steel specimens by coating with TH450 Chrome Nickel Amorphous using wire arc spray and to compare the cooling rates of specimens under difference conditions. Mechanical testing was performed using Micro Vickers Hardness Tester for hardness measurement, which revealed that the average surface hardness ranged between 560-600 HV. HAZ of coated areas had different effects on cooling rate on SCCW and SCCNT specimens which showed the hardness between 155–160 HV and also showed slightly changes in microstructure. While SCCO and SCCS specimens were most affected by heat, their hardness decreased and ranged between 80-90 HV. The tensile test of uncoated and coated specimens cooled under different conditions was then conducted and it was found that the ultimate tensile strength of plain specimens was 283.35 MPa which was slightly different. However, %elongation of coated specimen was higher than that of all other specimens. On the other hand, notched and coated specimen showed the ultimate tensile strength of 342.41 MPa and was higher compared to those of all uncoated specimens. However, %elongation showed no difference. According to One-Way ANOVA, P-value in F-test was 0.000 which was statistically significant at a level of 0.01. Tukey's multiple comparison test results and confidence levels showed the differences which were found that spray coating increased % elongation and tensile strength.

**Keywords:** wire arc spray; JIS G3141 SPCC steel; mechanical test; plain specimen; notched specimen.

## 1. INTRODUCTION

JIS G3141 cold rolled steel sheet has been used as important components in industrial applications such as manufacturing of parts for electrical appliances, air conditioner, refrigerator, washing machine, rice cooker, electric fan and compressor. It has also been used in automotive and aerospace industries [1, 2, 3] as base steel sheet (SPCC, SPCD, SPCE, SPCEN) or as cold rolled base steel sheet. The selection of steel sheets depends on the quality, grade and standards applied according to specification of the steel specimens to be assembled as a finished product. The advantages of using steel sheet as raw material are low cost and light weight. In addition, its quality can be improved by heat treatment and it can be compressed and bent into desired shapes. Steel sheet coms in a large single sheet and is also suitable for welding applications requiring high tensile strength and good load-bearing [4, 5]. The disadvantages are corrosive prone in areas with high humidity, but it depends on the potentiodynamic value [6, 7, 8]. High heat also affects the steel sheet, causing elongation and eventually fracture [9, 10]. Steel sheet has been improved by coating with composites (LMCs) by bonding layers of two or more metals in alternate fashion [10]. More ductile layers can prevent breaking in the other less ductile layers, thus coating the latter layers can improve its deformation beyond the peak tensile strain of each metal [11, 12, 13]. High velocity oxygen fuel (HVOF) coating has also been used by spraying WC-12Co powder on specimen surface, forming the coating layer with fine structure, high hardness, microporous and good mechanical properties. However, the disadvantage is the high cost of spraying machine [14, 15, 16, 17].

In this study, mechanical properties of JIS G3141 cold rolled steel sheet were improved using wire arc spray coating technique. In this spray coating, 2 wires were used as electrodes in an electrical circuit. These 2 wires were fed from each side of a spray gun and the end of each wire touched each other in front of the spray gun. Once electricity was applied through the wires, an electric arcing appeared at the wire ends in front of the spray gun. The wires were molten into fine powder particles and were pushed at high speed by compressed air and then adhered on the surface to be coated. It hardened and formed a layer of coating. The effects of changes in materials on mechanical properties were then studied.

## 2. Experimental Procedure

### 2.1 Materials

In this study, JIS G3141 SPCC cold rolled steel sheet manufactured according to American Welding Standard (AWS) was used. The steel sheet has maximum percentage of carbon (C), manganese (Mn) and phosphorus (P) of 0.15, 0.60 and 0.050%, respectively.

### 2.2 Specimen Preparation

Different specimens were prepared which included (a) plain specimens and (b) notched specimens with a hole of 2 mm at the center according to E (DIN 20125) standard [18]. The appearance and size of the specimen are as shown in (Figure-1). The specimens used

VOL. 16, NO. 20, OCTOBER 2021 ISSN 1819-6608
ARPN Journal of Engineering and Applied Sciences



in this study have 155±1 mm length (Lt), 5 mm thick (a), 16±1 mm width and 50±1mm gauge length (Lo).

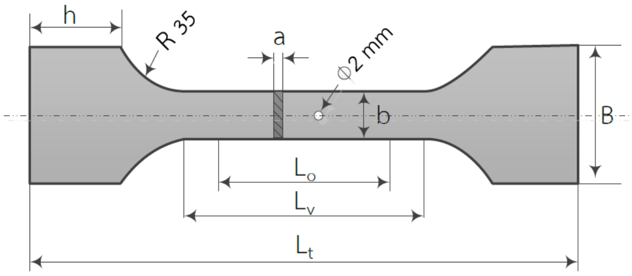


**Figure-1.** Specimen used in mechanical testing.

## 2.3 Experimental Design

**a) Wire arc spray coating:** In this study, spray coating was performed using wire arc spray machine, model AH 20A with 20HP-15KW air compressor as shown in (Figure-2) [18] and with the parameters as shown in Table-1. Before spray coating, rust and oil stains on the specimen surface were removed by sandblasting. After that, the specimens were spray coated with TH205 Nickel Aluminum in order to increase adhesion and then spray coated with TH450 Chrome Nickel Amorphous in order to increase specimen strength.

**Figure-2.** Wire arc spray, model AH 20A.

**Table-1.** Control parameters used in spray coating.

| No. | Parameter | Default value | Unit |
|---|---|---|---|
| 1. | Air compressor, 20 HP/15 KW, model AH 20A | 8 | Bar |
| 2. | Voltage | 37.5 | V |
| 3. | Electric current flowing through a conductor | 19.6 | A |
| 4. | Temperature up to | 1700 | °F |

**b) Cooling efficiency test:** Cooling efficiency under different conditions was studied. Specimens were first spray coated with primer and then TH450 Chrome Nickel Amorphous. After spray coating, the specimens were immediately cooled under different conditions such as cool in water (CW), cool in oil (CO), cool in salt (CS), and cool in normal temperature (CNT).

## 2.4 Microstructural Analysis

Before microstructural analysis, the specimens were polished using 80, 100, 240, 400, 600, 800, 1000, 1200, 1500, 2000 grit sandpapers and finished using 6, 3, 2 µm felt cloth. The specimens were then etched with the mixture of nitric acid in alcohol for 5 minutes. The effects on specimens such as uncoated specimen (SN), spray coated specimen cooled in cool water (SCCW), spray coated specimen cooled in oil (SCCO), spray coated specimen cooled in salt (SCCS), and spray coated specimen cooled in normal temperature (SCCNT) were studied. Microstructural analysis was performed using View Met Inverted Microscope, model NIB-100 in order to study the effects of cooling conditions on uncoated coated specimens at the heat affected zone (HAZ) of wire arc spray coated areas.

## 2.5 Hardness Test using Vickers Hardness Tester

Hardness of SN, SCCW, SCCO, SCCS and SCCNT were determined using Micro Vickers Hardness Tester with 500 g compression load for 10 seconds per point. Hardness values were measured at 10 points according to section D Before hardness test, the specimens were polished to expose their microstructure and 5 of 15 polished specimens were randomly selected and used in hardness test.

**a) Tensile testing:** The mechanical properties of SN, SCCW, SCCO, SCCS and SCCNT were then studied. The specimens used in this tensile testing are showed in (Figure-1) which included plain specimens (PS), 2 mm notched specimen (NS). Tensile testing of specimens cooled under different conditions was performed at Disp of 0.500 mm/min, 1.00 kN/s or 10 MPa/s load and 0.05 mm/s extension speed in triplicate per treatment for a total of 30 specimens [19]. The average tensile strength was then calculated.

**b) One-way ANOVA:** One-way ANOVA is the determination of the difference between means of single independent variables or single factor. However, it is divided into 2 or more groups and Tukey's multiple comparison test was then performed [20].

VOL. 16, NO. 20, OCTOBER 2021 ISSN 1819-6608
ARPN Journal of Engineering and Applied Sciences

www.arpnjournals.com

## 3. RESULTS

### 3.1 Hardness Test under Different Conditions

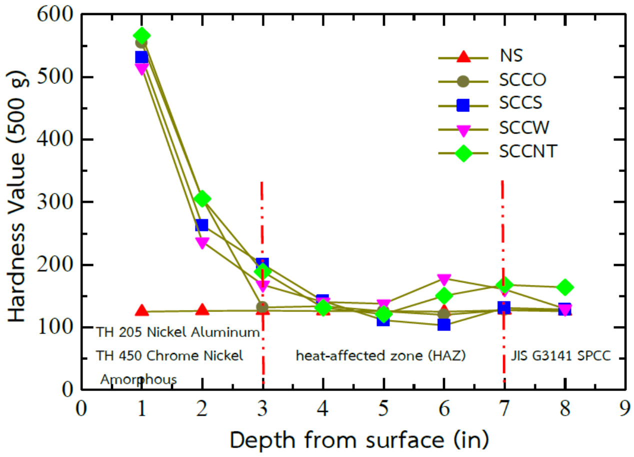


**Figure-3.** Comparison of hardness values of specimens.

Figure-3 represents tensile testing of JIS G3141 SPCC steel coated with TH450 Chrome Nickel Amorphous and cooling under different conditions. It was found that Point 1-2 of coated specimens showed higher hardness compared to that of all uncoated specimens. The areas coated with Chrome Nickel Amorphous had similar high surface hardness in the range of 560-600HV, since all 4 specimens were spray coated simultaneously, which is consistent with [21, 22, 23]. However, in (Figure-3), the heat affected zones (HAZ) were observed at Point 3-7 of the specimens cooled under different conditions between the coating layer and specimen. As a result, the hardness values of SCCW and SCCNT ranged between 155-160HV at HAZ, similar to [24], which showed higher hardness because the hardness of SN ranged between 105-110HV and consistent with [25]. Hardness of HAZ of SCCO and SCCS ranged between 80-90HV, which showed the most heat affected. At Point 8, the specimens were slightly affected by heat and their hardness therefore they were not different from that of SN.

### 3.2 Microstructure Classification and Structural Observation

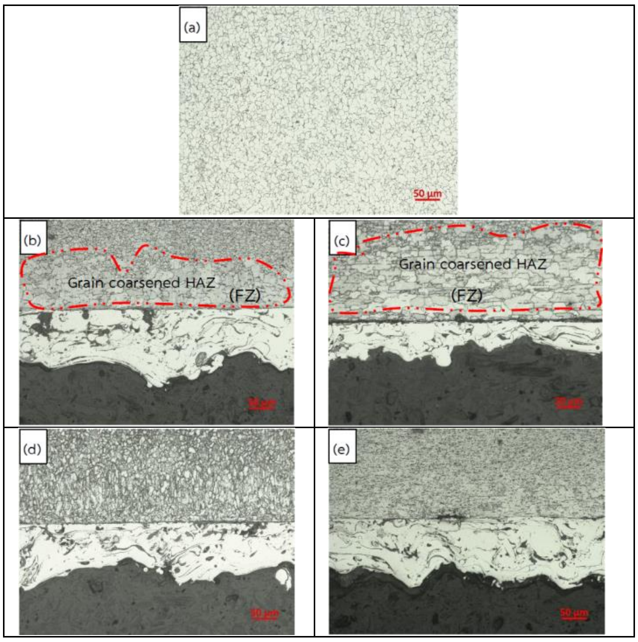


**Figure-4.** Microstructure of uncoated and coated specimens cooled under different conditions: (a) SN, (b) SCCO, (c) SCCS, (d) SCCW, and (e) SCCNT.

Microstructural analysis was performed using ViewMet Inverted Microscope. The results are shown in (Figure-4) (a). It was found that the cross-section of SN which is uncoated specimen was not affected by heat and did not show any deformation. For (Figure-4) (b), SCCO and (Figure-4) (c), SCCS, the microstructure between fusion zone (FZ) and coated specimen was affected by heat. Cooling in CO and CS resulted in high cooling rate. This resulted in change in microstructure into (α + Fe3C) and expansion of HAZ and coarsened grain due to HAZ caused by spray coating. The hardness values at Point 3-7 in (Figure-3) decreased and ranged between 80-90HV and was in line with (Figure-3). For the effects of heat on Fig. (d) CCW and Fig. (e) SCCNT, it was found that the microstructure between specimen and coated area, the cooling rate of these 2 specimens in fusion zone (FZ), was affected by heat. Cooling in CW and CNT resulted in higher hardness at fine grain microstructure. This is consistent with (Figure-3) which showed the structural components called perlite and ferrite. The hardness at HAZ at Point 3-7 in (Figure-3) ranged between 155-160HV which was higher than that of SN.

VOL. 16, NO. 20, OCTOBER 2021 ISSN 1819-6608
ARPN Journal of Engineering and Applied Sciences

www.arpnjournals.com

### 3.3 Tensile Test under Different Conditions

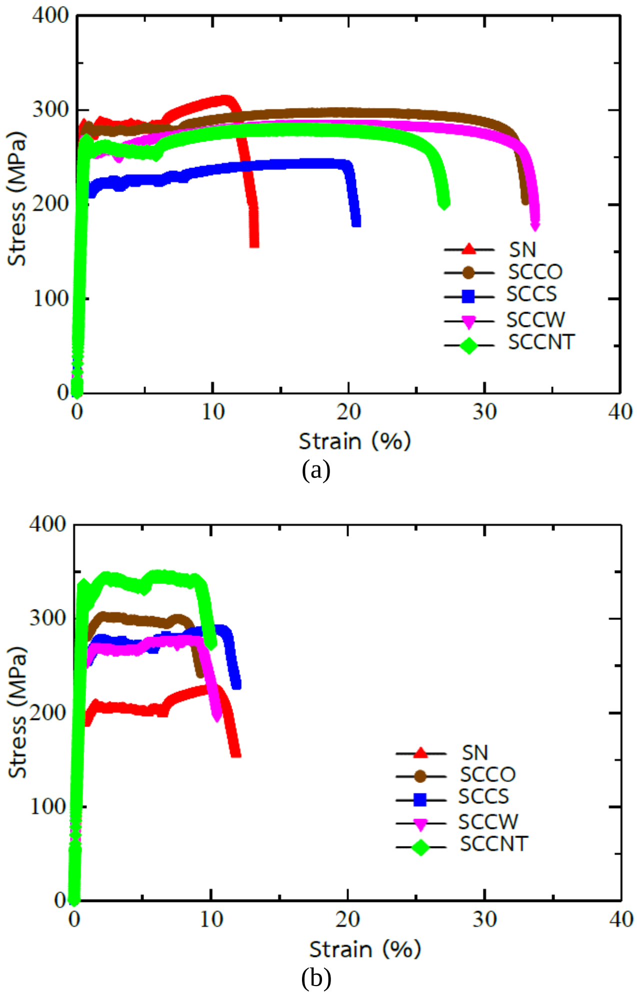


**Figure-5.** Comparison of Strain-Strength (a) PS and (b) NS, 5 specimens.

Comparison of tensile strength of (a) PS and (b) NS specimens in (Figure-5) revealed that tensile strength of both SN specimens and ultimate tensile strength of PS were 275.58 MPa which were not different from JIS G3141 SPCC steel and in line with [25]. NS showed ultimate tensile strength of 193.11 MPa which was lower PS than because it had 2 mm notch at the center as shown in (Figure-1) resulting in lower hardness and tensile strength.

Comparison of tensile strength of SCCO and SCCS revealed that both SN specimens showed tensile strength of 283.35 MPa and 216.85 MPa as shown in (Figure-5) (a) and (Figure-5) (b). Microstructure showed HAZ expansion which resulted in coarsened grain and HAZ as shown in (Figure-4) ($\alpha$ + $Fe_3C$) microstructure was observed. The material structure consists of a large number of atoms connected by bonds. When force was continuously applied to the specimen without interruption, this caused stress flow resulting in higher % elongation for both specimens. On the other hand, for SCCO and SCCS, both NS specimens which had 2 mm notch at the center showed tensile strength of 302.24 MPa and 277.41 MPa, respectively. In engineering, the notch prevents the stress flow, resulting in higher tensile strength and lower %elongation.

As for SCCW and SCCNT, it was found that tensile strength of both NS specimens were 285.61 and 282.12 MPa, respectively, resulting in high strength at fine grain structure which is consistent with (Figure-3). The material structure consists of many atoms connected by chemical bonds between atoms. When force was continuously applied to the specimen without interruption, this caused stress flow resulting in higher %elongation in both specimens. The structural components called perlite and ferrite were consistent with microstructure shown in (Figure-4) (d) and (e). On the other hand, both SCCW and SCCNT specimens showed tensile strength of 288.24 MPa and 342.41 MPa, respectively which had 2 mm notch at the center.

It can be observed that high heat was generated in specimens coated with chrome nickel amorphous resulting in hard surface. PS specimens showed orientation in material structure consisting of a large number of atoms connected by bonds between atoms. When force is continuously applied to the specimen without interruption, this caused stress flow resulting in higher %elongation in all specimens. As for NS specimens, when force was continuously applied, the stress arising in the affected region is transferred to adjacent atoms causing stress flow. When the stress flow is interrupted, it is necessary to change its direction several times, resulting in accumulation of stress concentration due to the discontinuity of the material. This decreased %elongation in all specimens. On the other hand, it resulted in higher tensile strength.

### 3.4 Tukey's Multiple Comparison Test and Confidence Interval

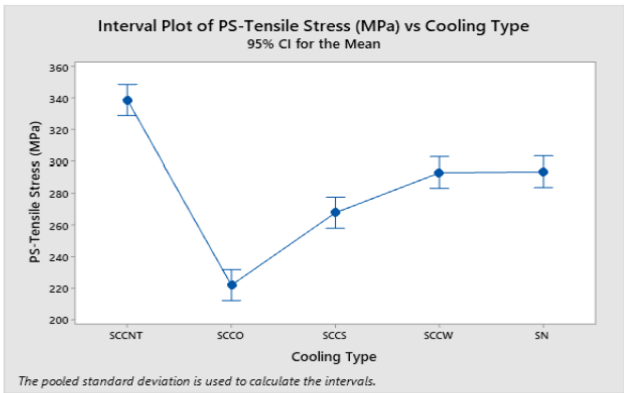


**Figure-6.** Confidence interval of PS vs tensile stress.

VOL. 16, NO. 20, OCTOBER 2021 ISSN 1819-6608
ARPN Journal of Engineering and Applied Sciences



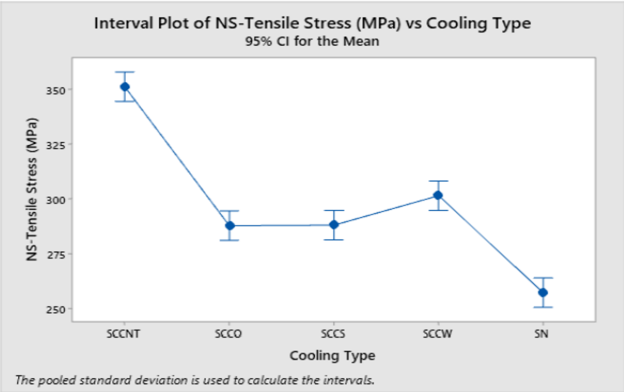


**Figure-7.** Confidence interval of NS vs tensile stress.

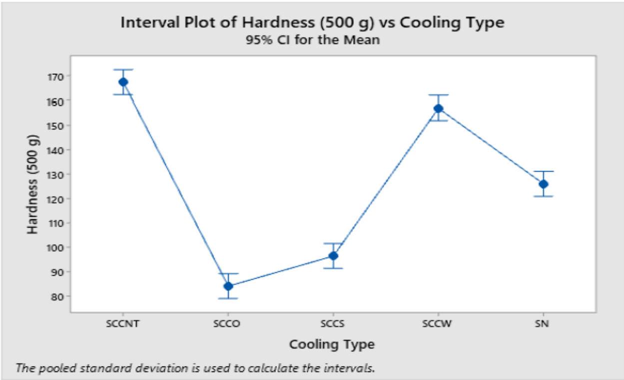


**Figure-8.** Confidence interval of hardness vs cooling condition.

The results of One-Way ANOVA revealed that P-value from F-test was 0.000 which showed statistical significance. This indicated that the cooling rates of PS versus tensile of all 5 specimens were different at a statistical significance level of 0.01. According to Tukey's multiple comparison test, it was found that the specimens could be classified into 4 groups in descending order of tensile strength as follows: SCCNT, SC and SCCW, SCCS and SCCO. The 95% confidence level of average tensile strength is shown in (Figure-6).The results are consistent with the experiment (Figure-5) (a)

(Figure-7) shows One-Way ANOVA results which revealed that P-Value from F-test was 0.000 which showed statistical significance. This indicated that the cooling rates of NS vs Tensile of all 5 specimens were different at a statistical significance level of 0.01. According to Tukey's multiple comparison test, it was found that the specimens could be classified into 4 groups in descending order of tensile strength as follows: SCCNT, SCCW and SCCS, SCCS and SCCO, and SN. The 95% confidence level of average tensile strength is shown in (Figure-7). The results are consistent with the experiment (Figure-5) (b)

(Figure-8) shows One-Way ANOVA results which revealed that P-Value from F-test was 0.000 which showed statistical significance. This indicated that the harness vs cooling condition of all 5 specimens were different at a statistical significance level of 0.01. According to Tukey's multiple comparison test, differences were observed between all 5 specimens. The descending order of tensile strength is as follows: SCCNT, SCCW, SN, SCCS, and SCCO. The 95% confidence level of average tensile strength is shown in (Figure-8).The results are consistent with the experiment (Figure-3)

## 4. CONCLUSIONS

Spray coating of JIS G3141 SPCC steel with TH450 Chrome Nickel Amorphous increased strength of specimens. After deterioration of the coating layer, the specimen can be re-sprayed for many times, thus saving maintenance costs.

- After arc spray coating, the specimens should not be cooled in CO and CS. This is because the effect of high heat will result in changes in microstructure ($\alpha$ + $Fe_3C$) due to HAZ resulting in coarsened grain and expansion of HAZ. This increased the strength of the specimens.
- For plain specimens, thermal effect of Chrome Nickel Amorphous coating resulted in slightly difference in tensile strength between coated and uncoated specimens while coated specimen showed higher %elongation compared to uncoated specimen.
- For notched specimens, thermal effect of Chrome Nickel Amorphous coating resulted in higher tensile strength in coated specimen compared to uncoated specimen while no difference in %elongation was observed between both specimens.

## 5. SUGGESTIONS

Spray coating increased the strength of specimens. After deterioration of the coating layer, the specimen can be re-sprayed for many times. This technique is therefore suitable for and can be applied to other materials such as other types of steel or aluminum. However, to ensure the effectiveness of this technique, more tests should be conducted.

According to the hardness test, as thickness of the coating layer increased the hardness of specimen increased, measuring from the outermost coating layer toward the innermost coating layer. Therefore, the speed should be optimized.

## ACKNOWLEDGMENT

We would like to thank Ratchawong Furniture Company Limited for supporting the materials used in this research and the Department of Industrial Engineering, Faculty of Engineering, Nakhon Phanom University for providing assistance in instrument testing in this research.

## REFERENCES

[1] Bosbach B., Ohle C., Fiedler B. 2018. Structural health monitoring of fibre metal laminates under mode I and II loading. Composites Part A: Applied Science and Manufacturing. 107: 471-478.

[2] Risonarta V. Y., Fadly H. A., Perdana H. F. 2017. Metallurgical Analysis of Steel Plate for Deep Drawing Application. International Journal of Industrial Research and Applied Engineering. 2(1): 25-28.

[3] ZAMRI R. B. 2016. Surface defect detection and polishing parameter optimization using image processing for G3141 cold rolled steel. (Doctoral dissertation, School of Graduate Studies, Universiti Putra Malaysia).

[4] Muflikhun M. A., Higuchi R., Yokozeki T. and Aoki T. 2020. Delamination behavior and energy release rate evaluation of CFRP/SPCC hybrid laminates under ENF test: Corrected with residual thermal stresses. Composite Structures. 236: 111890.

[5] Shimamoto K., Sekiguchi Y. and Sato C. 2016. Mixed mode fracture toughness of adhesively bonded joints with residual stress. International Journal of Solids and Structures. 102: 120-126.

[6] Kim Y., Yoo M. and Moon M. 2020. Effects of Surface Roughness on the Electrochemical Properties and Galvanic Corrosion Behavior of CFRP and SPCC Alloy. Materials. 13(18): 4211.

[7] Schulz M., Shanov V., Yin Z. andCahay M. (Eds.). 2019. Nanotube Superfiber Materials: Science, Manufacturing, Commercialization. William Andrew.

[8] Li S., Khan H. A., Hihara L. H., Cong H. and Li J. 2018. Corrosion behavior of friction stir blind riveted Al/CFRP and Mg/CFRP joints exposed to a marine environment. Corrosion Science. 132: 300-309.

[9] Muroya Y., Motoki A., Shimanoe K., Maeda T., Haruta Y., Teraoka Y. and Yamazoe N. 2006. Densification of SiO2-Al2O3-TiO2 based ceramic film coated on steel for high thermal stabilty and mechanical properties. Surface and Coatings Technology. 201(3-4): 880-885.

[10] Koshiba Y., Okazaki S. and Ohtani H. 2016. Experimental investigation of the fire extinguishing capability of ferrocene-containing water mist. Fire Safety Journal. 83: 90-98.

[11] Embury D., Bouaziz O. 2010. Steel-based composites: driving forces and classifications. Annual review of materials research. 40: 213-241.

[12] Nambu S., Michiuchi M., Inoue J. and Koseki T. 2009. Effect of interfacial bonding strength on tensile ductility of multilayered steel composites. Composites Science and Technology. 69(11-12): 1936-1941.

[13] Nambu S., Michiuchi M., Ishimoto Y., Asakura K., Inoue J. and KosekiT.2009. Transition in deformation behavior of martensitic steel during large deformation under uniaxial tensile loading. Scripta Materialia. 60(4): 221-224.

[14] Uyulgan B., Dokumaci E., Celik E., Kayatekin I., Azem N. A., Ozdemir I. and Toparli M. 2007. Wear behaviour of thermal flame sprayed FeCr coatings on plain carbon steel substrate. Journal of materials processing technology. 190(1-3): 204-210.

[15] Thermsuk S., Surin P. 2019. Optimization Parameters of WC-12Co HVOF Sprayed Coatings on SUS 400 Stainless Steel. Procedia Manufacturing. 30: 506-513.

[16] Brezinová J., Guzanová A., Mamuzic I. 2012. Study of wear resistance of coatings deposited by High Velocity Oxygen Fuel (HVOF) technology. Acta Metallurgica Slovaca. 18(1): 20-27.

[17] Tillmann W., Vogli E., Baumann I., Matthaeus G. and Ostrowski T. 2008. Influence of the HVOF gas composition on the thermal spraying of WC-Co submicron powders (− 8+ 1 μm) to produce superfine structured cermet coatings. Journal of thermal spray technology. 17(5-6): 924-932.

[18] Gedzevicius I., Valiulis A. V. 2006. Analysis of wire arc spraying process variables on coatings properties. Journal of Materials Processing Technology. 175(1-3): 206-211.

[19] Stange E., Khawaja H. 2018. IR Thermography of Steel Specimens undergoing Tensile Tests.

[20] Pohlert T. 2014. The pairwise multiple comparison of mean ranks package (PMCMR). R package. 27(2019): 9.

[21] Sangsuriyun M., Surin P., Eidhed K., 2020. Corrosion behavior of ASME SA-192 steel finned tube by wire arc spray in temperature control and high-salt environment. in Proc. 8th International Conference on Mechanical, Automotive and Materials Engineering, Ho Chi Minh City, Vietnam, Dec. 25-27.

[22] Sun X., Stephens E. V., Khaleel M. A. 2008. Effects of fusion zone size and failure mode on peak load and

energy absorption of advanced high strength steel spot welds under lap shear loading conditions. Engineering Failure Analysis. 15(4): 356-367.

[23] Ghazali F. A., Salleh Z., Hyie K. M., Rozlin N. N., Hamidi S. A. and Padzi M. M. 2017. Effect of post weld impact treatment (PWIT) on mechanical properties of spot-welded joint. In AIP Conference Proceedings (1901(1): 050004). AIP Publishing LLC.

[24] Joy-A-Ka S., Hirano T., Akebono H., Kato M. and Sugeta A. 2013. Fatigue properties and crack growth behavior of friction stir spot welded 300 MPa-class automobile steel sheets. In Proceedings of the 9th International Conference on Fracture & Strength of Solids. Vol. 9.

[25] Muflikhun M. A., Chua A. Y. 2020. Load-displacement experimental data from axial tensile loading of CFRP-SPCC hybrid laminates. Data in brief. 29: 105306.